European Journal of Radiology 118 (2019) 66–74

Contents lists available at ScienceDirect

European Journal of Radiology

journal homepage: www.elsevier.com/locate/ejrad

Research article

Liver MRI susceptibility-weighted imaging (SWI) compared to T2* mapping in the presence of steatosis and fibrosis

Verena C Obmann[a], Christina Marx[a], Annalisa Berzigotti[b], Nando Mertineit[a], Joris Hrycyk[a], Christoph Gräni[c], Lukas Ebner[a], Michael Ith[a], Johannes T Heverhagen[a], Andreas Christe[a,1], Adrian T Huber[a,*,1]

[a] Department of Diagnostic, Interventional and Pediatric Radiology, Inselspital, Bern University Hospital, University of Bern, Bern, Switzerland
[b] Hepatology, Department of Visceral Surgery and Medicine, Inselspital, Bern University Hospital, University of Bern, Bern, Switzerland
[c] Department of Cardiology, Inselspital, Bern University Hospital, University of Bern, Bern, Switzerland

ARTICLE INFO

Keywords:
T2* mapping
Susceptibility weighted imaging
Magnetic resonance elastography
Proton density fat fraction
Liver steatosis
Hepatic fibrosis

ABSTRACT

Purpose: To show that both susceptibility-weighted imaging (SWI) and T2*-mapping are dependent on liver steatosis, which should be taken into account when using these parameters to grade liver fibrosis and cirrhosis.
Methods: In this prospective study, a total of 174 patients without focal liver disease underwent multiparametric MRI at 3 T including SWI, T1- and T2* mapping, proton density fat fraction (PDFF) quantification and MR elastography. SWI, T2* and T1 were measured in the liver (4 locations), as well as in paraspinal muscles, to calculate the liver-to-muscle ratio (LMR). Liver and LMR values were compared among patients with different steatosis grades (PDFF < 5%, 5–10%, 10–20% and > 20%), patients with normal, slightly increased and increased liver stiffness (< 2.8 kPa, 2.8–3.5 kPa and > 3.5 kPa, respectively). ANOVA with Bonferroni-corrected post hoc tests as well as a multivariate analysis were used to compare values among groups and parameters.
Results: SWI and T2* both differed significantly among groups with different steatosis grades ($p < 0.001$). However, SWI allowed a better differentiation among liver fibrosis grades ($p < 0.001$) than did T2* ($p = 0.05$). SWI LMR ($p < 0.001$) and T2* LMR ($p = 0.036$) showed a similar performance in differentiating among liver fibrosis grades.
Conclusion: SWI and T2*-mapping are strongly dependent on the liver steatosis grades. Nevertheless, both parameters are useful predictors for liver fibrosis when using a multiparametric approach.

1. Introduction

Imaging-based detection and quantification of diffuse liver disease represents a noninvasive surrogate for liver biopsies and allows repetitive, longitudinal follow-up and therapy guidance [1]. The current noninvasive reference standard for liver fibrosis quantification is magnetic resonance (MR) elastography [2,3], which allows the analysis of the entire liver volume with a high interreader reliability and accuracy [4,5] compared to histology [6]. However, MR elastography is expensive and restricted to experienced tertiary centers [3,7], thus, other noninvasive tools are of the utmost interest for grading liver fibrosis.

MR T2*-mapping is widely used to noninvasively quantify the liver iron content in patients with hemochromatosis or thalassemia [8,9], since the T2* relaxation time is shortened by iron due to B0 inhomogeneities [10]. However, an increased liver iron content also represents an important background alteration in liver fibrosis [11], since cirrhotic nodules contain hemosiderotic depositions [12] and increasing fibrosis stages are correlated with serum ferritin and liver iron content [13]. Wang et al. showed that a decreased T2* relaxation time is associated with an increase in the Child-Pugh classes in liver cirrhosis [14], while Guimares et al. showed a similar association in precirrhotic stages of fibrosis [15].

Using a similar approach, susceptibility weighted imaging (SWI) is

Abbreviations: ALP, alkaline phosphatase; ALT, alanine aminotransferase; APRI, AST to platelet ratio index; AST, aspartate aminotransferase; BMI, body mass index; CT, computed tomography; GGT, gamma-glutamyl transpeptidase; GRE, gradient recalled echo; ICC, intraclass correlation; INR, international normalized ratio; MRI, magnetic resonance imaging; PDFF, proton density fat fraction; ROI, region of interest; SI, signal intensity; SWI, susceptibility weighted imaging

* Corresponding author at: Department of Diagnostic, Interventional and Pediatric Radiology, Freiburgstrasse 10, Inselspital, 3010 Bern, Switzerland.
E-mail address: Adrian.huber@insel.ch (A.T. Huber).

[1] These authors contributed equally to this work.

https://doi.org/10.1016/j.ejrad.2019.07.001
Received 28 March 2019; Received in revised form 22 June 2019; Accepted 1 July 2019

based on a gradient-echo (GRE) technique that utilizes both magnitude and phase information to increase the sensitivity for paramagnetic substances [16]. SWI is routinely used to detect microhemorrhages in the brain [17–19], but recent technical advances have allowed for abdominal applications as well [20–22]. Zhang et al. demonstrated that SWI could provide quantitative evaluation of renal fibrosis [23]. Balassy et al. showed that an increased SWI liver to muscle ratio (LMR) correlates with an increasing liver fibrosis grade [24]. Other groups have shown similar results for SWI in rabbits with induced liver fibrosis [25,26]. One possible explanation are iron deposits in siderotic nodules, another hypothesis is that SWI is highly sensitive to fibrotic alterations in the interstitial matrix. Both SWI and T2* can be easily performed in any Radiology department and do not need specific equipment such as MR elastography. Those parameters represent interesting tools to characterize liver fibrosis in combination with other MR imaging sequences.

Few studies have compared SWI and T2* in the liver in the presence of steatosis. There is evidence that both SWI and T2* values are influenced by intrahepatic fat [27–29]. Since patients with diffuse liver disease often have coexistent liver steatosis [10,30,31], particularly in the context of non-alcoholic fatty liver disease, more detailed knowledge about the effect of liver fat and liver fibrosis on SWI- and T2*-values is needed in order to differentiate between patients with and without liver fibrosis.

The purpose of this study is to assess if SWI and T2*-mapping are dependent on liver steatosis, which should be taken into account when using these parameters to stage liver fibrosis in patients with chronic liver disease.

2. Material and methods

2.1. Study population

This prospective cross-sectional Health Insurance Portability and Accountability (HIPAA) compliant study was approved by the local ethic commission (Kantonale Ethikkommission Bern, IRB number 282/15) and was conducted after obtaining the patient's written informed consent. We consecutively included 184 study participants without focal liver disease (no solid lesion > 1 cm), based on abdominal computed tomography (CT) scans, without prior transjugular intrahepatic portosystemic shunt (TIPS) or prior liver surgery. Excluded were 10 patients, due to portal vein thrombosis (n = 4), insufficient MRE quality (n = 5) and abortion of MRI exam due to claustrophobia (n = 1) (Fig. 1). There were no patients with iron overload (hemochromatosis/thalassemia) in our study population. Indications for CT scans varied between: trauma scans (n = 25), search for non-liver related tumors (n = 45), acute abdomen (n = 27), search for infection focus (n = 36) and HCC screening (n = 26). In 15 participants, focal liver disease has been excluded based on MRI. There was no known history of liver disease in the patients with liver stiffness < 2.8 kPa. Out of 51 patients with increased liver stiffness > 2.8 kPa, 15 patients had viral hepatitis, 10 patients had an alcoholic liver disease and 10 patients presented with NAFLD/NASH. Therefore, 16 patients had no known history of chronic liver disease.

Enrolled patients underwent multiparametric MR imaging at 3 T in our institution between 03/2016 and 02/2018, including SWI, T2* and T1 mapping, proton density fat fraction (PDFF) quantification and MR elastography. Patients were divided into three groups based on the liver stiffness as measured on MR elastography stiffness maps by a radiologist with 8 years of experience in liver imaging (A.T.H.) who was blinded to the patient's clinical history: normal liver stiffness (shear modulus < 2.8 kPa, n = 123), slightly increased liver stiffness (shear modulus 2.8–3.5 kPa, n = 21) and increased liver stiffness (shear modulus > 3.5 kPa, n = 30). These cutoffs correspond to Metavir fibrosis stages of F0, F1 and ≥ F2, respectively) [6]. Patients with normal liver stiffness were then grouped based on their liver fat content as measured by the same radiologist per the PDFF (< 5%, 5–10%, 10–20%, > 20%, n = 38, 59, 19 and 7, respectively) [30,32]. Clinical information and laboratory test results were recorded. The clinical parameters included age, gender, body mass index (BMI),history of diabetes or hypertension, tobacco use and alcohol consumption. Biological parameters included dyslipidemia, platelet count, quick value, total bilirubin levels, gamma-glutamyl transpeptidase (GGT), aspartate aminotransferase (AST), alanine aminotransferase (ALT), alkaline phosphatase, albumin, creatinine, hematocrit and serum ferritin level.

2.2. MR imaging technique

Patients were examined with a 3 T-MR system (Verio, Siemens Healthineers, Erlangen, Germany) in a fasting state (4 h prior to exam). For T2* mapping, a multiecho gradient echo (GRE) single breath-hold sequence (12 echoes with an echo time (TE) between 0.93–14.2 ms, repetition time (TR) of 200 ms, flip angle (FA) 18°, field-of-view (FOV) 400, 10 mm slice thickness) was performed and T2* maps were generated on three single slices in the upper, mid and lower liver. For susceptibility weighted imaging we used a 3D GRE-based SWI sequence (TE of 20 ms, TR of 27 ms, in-plane resolution of 2.1 x 1.4 mm, and a through-plane resolution of 4 mm with 10% slice oversampling, FOV 350, FA 15°). T1 mapping was acquired with an axial MOLLI single breath-hold sequence (TE of 1.01 ms, TR of 740 ms, inversion time (TI) 225 ms, FA 35°, 8-mm slice thickness, FOV (FOV) 384, matrix 154 × 192 pixels). Diffusion weighted imaging was performed using a TR of 3200 ms, TE of 53.2 ms, slice thickness of 5 mm with b-values of 50, 180 and 700 s/mm [2] and calculation of apparent diffusion coefficient (ADC) maps.

All exams were performed using a body array coil. The PDFF was calculated using the Dixon method with axial T1-weighted VIBE images (TE of 2.45 ms and 3.68 ms, TR of 5.47 ms, FA 9°, 3 mm slice thickness, and scan time of 22 s) to differentiate patients with and without liver steatosis. For MR elastography, a pneumatic driver (Resoundant, Rochester, MN, USA) was placed on the right upper quadrant, transmitting shear waves by continuous acoustic vibrations with a frequency of 60 Hz. The liver shear stiffness in kPa in the right liver lobe was determined with a gradient echo-based elastography sequence on 3 single-slice acquisitions with 5 mm slice thicknesses using the 95% confidence map of stiffness. A shear modulus ≥ 2.8 kPa and < 3.5 kPa was considered to represent a slightly increased liver stiffness (corresponding to histology fibrosis grade F0-F1, according to the Metavir staging system), while a shear modulus ≥ 3.5 kPa was defined as liver fibrosis (corresponding to clinically significant liver fibrosis with histology fibrosis grade ≥ F2) [3,6,33].

2.3. MR image analysis

Corresponding to methods published before [24], 4 polygonal regions of interest (ROI) were drawn on the SWI images in the segments of the left (II/III, IVa/IVb) and right (VII/VI, VIII/VI) liver on the level of the portal vein by two others radiologists with 6 and 3 years of experience in liver imaging (V.C.O. and N.M.) who were also blinded to the patient's clinical history. Large vessels, bile ducts and partial volume, including air or perihepatic fat at the liver border were excluded. In addition, 2 ROI were drawn on both sides in the paravertebral muscles on the level of the liver, and the liver-to-muscle ratios for each parameter were calculated using the mean values. The same measurements were performed on the T2*- and T1- maps. The mean ROI size was 685 ± 203 mm^2 [2]. The shear modulus (in kPa) on MR elastography images and PDFF (in %) in the right liver were measured on three slices, using polygonal ROIs. The median value of the three ROIs was then calculated.

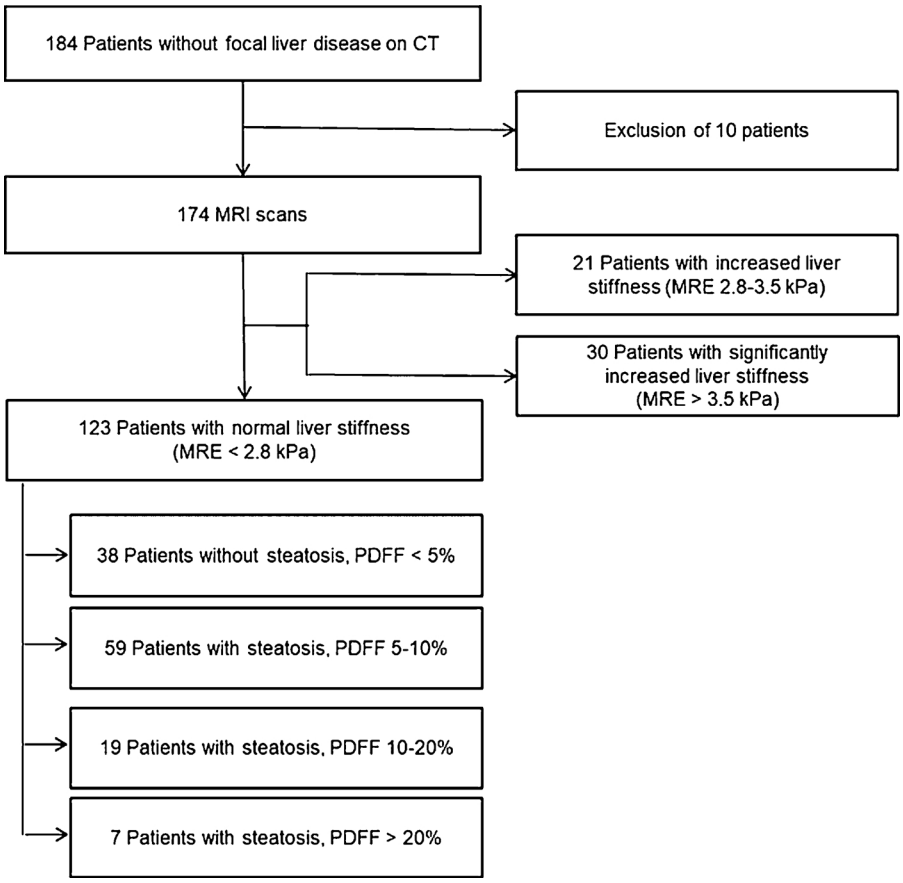

Fig. 1. Study participants workflow chart.
184 patients without focal liver disease on CT were included. Excluded were 10 patients, due to portal vein thrombosis (n = 4), non diagnostic MRE quality (n = 5) and abortion of MRI exam due to claustrophobia (n = 1). Of the 174 patients included in analysis, 123 patients had normal liver stiffness (shear modulus < 2.8 kPa), 21 had slightly increased liver stiffness (shear modulus 2.8–3.5 kPa) and 30 patients had at least moderately increased liver stiffness (shear modulus > 3.5 kPa). Patients with normal liver stiffness were grouped based on the degree of steatosis: n = 38 with PDFF < 5%, n = 59 5–10%, n = 19 10–20% and n = 7 > 20%.
CT = Computed tomography, MRI = Magnetic resonance imaging, PDFF = Proton density fat fraction, MRE = MR elastography, kPa = kilo Pascal.

Table 1
Baseline Characteristics based on liver stiffness.

	< 2.8 kPa		2.8-3.5 kPa		> 3.5 kPa		P-value
	Mean ± SD	n	Mean ± SD	n	Mean ± SD	n	
Male	48%	59/123	71%	15/21	60%	18/30	0.095
Age, years (all)	49 ± 15	123	58 ± 14	21	58 ± 10	30	0.002
Age, years (male)	52 ± 15	59	58 ± 15	15	56 ± 11	18	0.269
Age, years (female)	46 ± 14	64	57 ± 15	6	60 ± 7	12	< 0.001
BMI, kg/m [2]	26 ± 7	119	29 ± 6	21	29 ± 7	26	0.001
Tobacco	16%	20/123	33%	7/21	60%	18/30	< 0.001
Alcohol	6%	7/123	29%	6/21	70%	21/30	< 0.001
Arterial hypertension	16%	20/123	33%	7/21	47%	14/30	0.007
Chronic renal insufficiency	1%	1/123	0%	0/21	3%	1/30	0.444
Dyslipidemia	7%	9/123	33%	7/21	13%	4/30	0.002
Diabetes	5%	6/123	19%	4/21	30%	9/30	< 0.001
≥ 1 drug daily	21%	26/123	29%	6/21	60%	18/30	< 0.001
≥ 2 drugs daily	6.5%	8/123	15%	3/21	43%	13/30	< 0.001
Creatinine, µmol/l	79 ± 21	78	82 ± 18	18	77 ± 22	27	0.374
AST, U/l	28 ± 17	45	33 ± 22	13	48 ± 23	24	< 0.001
ALT, U/l	34 ± 38	59	58 ± 74	17	42 ± 29	24	0.004
GGT, U/l	40 ± 47	52	49 ± 36	16	160 ± 135	25	< 0.001
Alkaline phosphatase, U/l	74 ± 32	44	70 ± 24	14	107 ± 53	23	0.015
Bilirubin, µmol/l	10 ± 7	39	8 ± 4	13	25 ± 19	24	< 0.001
Albumin	36 ± 7	32	33 ± 5	10	33 ± 7	25	0.043
Quick, %	97 ± 11	54	94 ± 14	13	74 ± 19	24	< 0.001
APRI	0.53 ± 1.28	24	0.26 ± 0.33	11	1.70 ± 1.90	17	< 0.001
Ferritin	213 ± 348	29	222 ± 170	7	269 ± 208	22	0.177

Values represent the percentage, mean ± SD or n. P-values were calculated using the Mann-Whitney U or Fisher's exact test, as appropriate.
BMI = body mass index; HDL = high-density lipoproteins, LDL = low-density lipoproteins, AST = aspartate aminotransferase; ALT = alanine aminotransferase; GGT = gamma-glutamyl transferase; INR = International normalized ratio, evaluating the extrinsic pathway of coagulation, APRI = aspartate aminotransferase-to-platelet ratio index.

Table 2
Baseline characteristics based on PDFF in patients with normal liver stiffness.

	< 5%		5-10%		10-20%		> 20%		p-value
	Mean ± SD	n	Mean ± SD	n	Mean ± SD	n	Mean ± SD	n	
Male	45%	17/38	46%	27/59	58%	11/19	57%	4/7	0.256
Age, years (all)	43 ± 13	38	50 ± 16	59	55 ± 11	19	58 ± 12	7	0.005
Age, years (male)	45 ± 16	17	55 ± 15	27	56 ± 10	11	56 ± 14	4	0.189
Age, years (female)	42 ± 11	21	45 ± 16	32	54 ± 13	8	62 ± 10	8	0.043
BMI, kg/m [2]	24 ± 4	35	26 ± 9	58	28 ± 5	19	32 ± 4	7	< 0.001
Tobacco	21%	8/38	17%	10/59	11%	2/19	0%	0/7	0.410
Alcohol	2.6%	1/38	6.8%	4/59	11%	2/19	0%	0/7	0.564
Arterial hypertension	16%	6/38	12%	7/59	37%	7/19	14%	1/7	0.172
Chronic renal insufficiency	0%	0/38	1.70%	1/59	0%	0/19	0%	0/7	0.779
Dyslipidemia	2.6%	1/38	48%	7/59	5.3%	1/19	0%	0/7	0.296
Diabetes	5.3%	2/38	1.70%	1/59	5.3%	1/19	29%	2/7	0.021
≥ 1 drug daily	18%	7/38	23%	14/59	21%	4/19	5.7%	1/7	0.896
≥ 2 drug daily	2.6%	1/38	8.5%	5/59	5.3%	1/19	14%	1/7	0.56

Values represent the percentage, mean ± SD or n. P-values were calculated using the Mann-Whitney U or Fisher's exact test, as appropriate.
PDFF = Proton density fat fraction, BMI = body mass index; HDL = high-density lipoproteins, LDL = low-density lipoproteins, AST = aspartate aminotransferase; ALT = alanine aminotransferase; GGT = gamma-glutamyl transferase; INR = International normalized ratio, evaluating the extrinsic pathway of coagulation, APRI = aspartate aminotransferase-to-platelet ratio index.

Table 3
Comparison of SWI, T2* and T1 with and without the muscle ratio in patients according to liver stiffness.

	Liver shear modulus					Post hoc tests	
	< 2.8 kPa Mean ± SD	2.8-3.5 kPa Mean ± SD	> 3.5 kPa Mean ± SD	ANOVA p-value	< 2.8 vs. 2.8-3.5 kPa p-value	< 2.8 vs. > 3.5 kPa p-value	2.8-3.5 vs. > 3.5 kPa p-value
SWI Liver	84 ± 32	71 ± 27	46 ± 29	< 0.001	0.388	< 0.001	0.051
SWI L/M (%)	81 ± 27	66 ± 21	45 ± 26	< 0.001	0.105	< 0.001	0.074
T2* Liver	19 ± 5	17 ± 3	17 ± 4	0.050	0.298	0.127	1.000
T2* L/M (%)	86 ± 24	76 ± 17	69 ± 19	0.036	0.613	0.052	1.000
T1 Liver	780 ± 84	806 ± 125	919 ± 85	< 0.001	1.000	< 0.001	< 0.001
T1 L/M (%)	72 ± 11	75 ± 11	87 ± 10	< 0.001	0.564	< 0.001	0.004

Mean values and standard deviations are presented for signal intensities of SWI and for parametric values of T2* and T1 in ms in the liver as well as their liver-to-muscle ratio (demonstrate as %) for different patient groups depending on their liver stiffness grade measured as shear modulus in kPa (< 2.8 kPa, 2.8–3.5 and > 3.5 kPa). ANOVA with Bonferroni corrected post hoc tests was used for statistical testing.
SD = Standard deviation, SWI = susceptibility weighted imaging, L/M = Liver-to-muscle ratio.

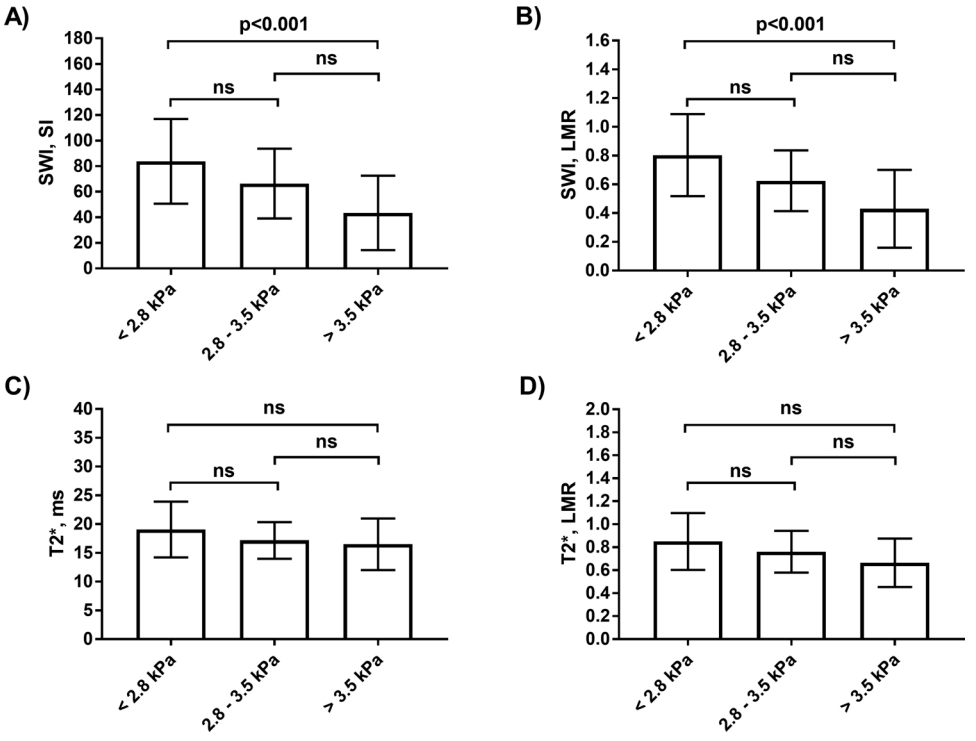

Fig. 2. SWI and T2* values in different fibrosis groups.
Column diagram of SWI liver values (A), SWI liver to muscle ratio (LMR) values (B), T2* liver values (C) and T2* LMR values (D) for stiffness groups < 2.8 kPa, 2.8–3.5 kPa and > 3.5 kPa. Differences between the SWI SI and SWI LMR results in the stiffness groups < 2.8 kPa and > 3.5 kPa were statistically significant ($p < 0.001$, ANOVA with Bonferoni corrected post hoc tests) while other group comparison or results in T2* liver and T2* LMR were not.
SWI = susceptibility weighted imaging, LMR = liver to muscle ratio, IQR = Interquartile range.

Table 4
Comparison of SWI, T2* and T1 with and without the muscle ratio in patients with normal liver stiffness, but with different degrees of steatosis.

	Patients with normal liver stiffness (< 2.8 kPa)				ANOVA	Post hoc tests					
	PDFF					PDFF					
	< 5%	5-10%	10-20%	> 20%		< 5 vs. 5-10%	< 5 vs. 10-20%	< 5 vs. > 20%	5-10 vs. 10-20%	5-10 vs. > 20%	10-20 vs. > 20%
	Mean ± SD	Mean ± SD	Mean ± SD	Mean ± SD	p-value	p-value	p-value	p-value	p-value	p-value	p-value
SWI Liver	98 ± 30	89 ± 26	65 ± 33	42 ± 16	< 0.001	0.862	< 0.001	< 0.001	0.012	0.012	0.400
SWI L/M (%)	92 ± 26	85 ± 22	62 ± 27	47 ± 19	< 0.001	1.000	< 0.001	< 0.001	0.005	0.003	1.000
T2* Liver	22 ± 4	19 ± 5	17 ± 4	15 ± 2	< 0.001	0.001	< 0.001	< 0.010	0.864	0.091	1.000
T2* L/M (%)	96 ± 24	87 ± 23	72 ± 18	69 ± 16	0.009	0.793	0.022	0.101	0.267	0.539	1.000
T1 Liver	812 ± 72	756 ± 77	786 ± 88	899 ± 45	< 0.001	0.005	1.000	0.039	0.882	< 0.001	0.006
T1 L/M (%)	74 ± 13	69 ± 9	72 ± 8	78 ± 6	0.084	0.295	1.000	1.000	1.000	0.248	1.000

Mean values and standard deviations are presented for signal intensities of SWI and parametric values of T2* and T1 in ms as well as their liver-to-muscle ratio for different patient groups depending on their steatosis grade based on PDFF quantification (< 5%, 5–10%, 10–20% and > 20%). ANOVA with Bonferroni corrected post hoc tests was used for statistical testing.
SD = Standard deviation, SWI = susceptibility weighted imaging.

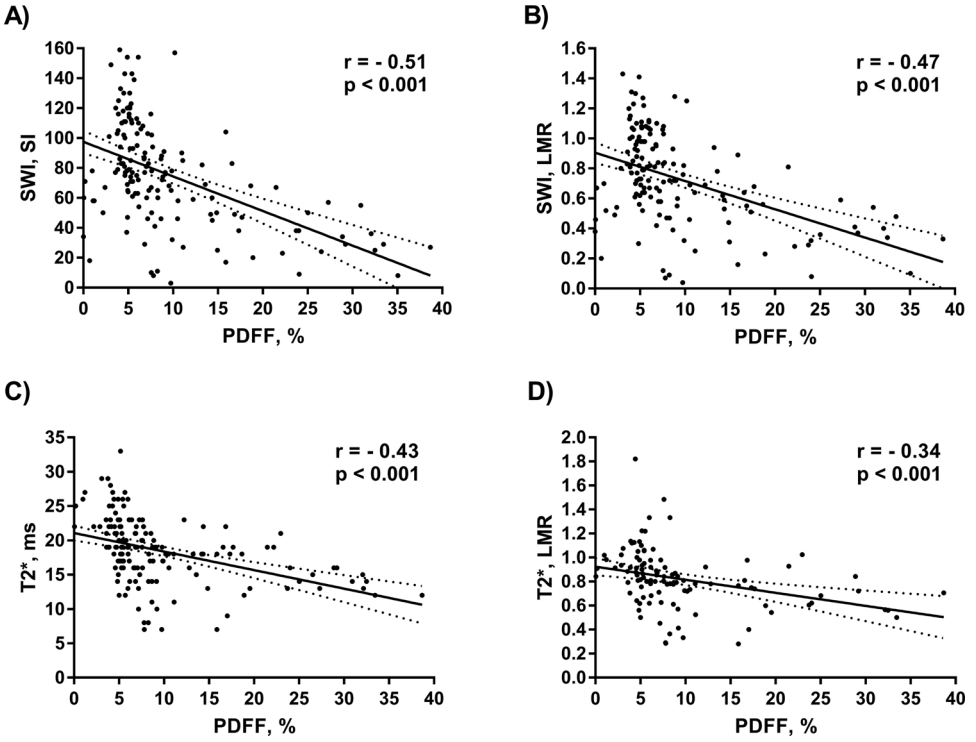

Fig. 3. Correlation among degree of steatosis and T2* and SWI.
Comparison of A) SWI and PDFF and C) T2* and PDFF with a significant correlation (r = -0.51, p < 0.001 and r = -0.43, p < 0.001, respectively). Correlating LMRs in B) SWI LMR and D) T2* LMR do show significant correlation as well, however with smaller correlation coefficients (r = -0.47, p < 0.001 and r = -0.34, p < 0.001, respectively).
PDFF = Proton density fat fraction, SWI = susceptibility weighted imaging, SI = Signal intensity.

2.4. Statistical analysis

The analysis was performed with the statistical software package R (version 3.4.1, R Foundation for Statistical Computing, Vienna, Austria) [19] and GraphPad Prism (Version 7.1, GraphPad Software Inc., La Jolla, CA, USA). The clinical characteristics (baseline characteristics and laboratory blood results as described in the section "study population") were compared among groups using the Wilcoxon test for continuous variables or Fisher's exact test for categorical variables. The p-value for significance was < 0.05.

ANOVA type II analysis with post hoc multiple comparisons of the means (Tukey Contrasts with Bonferroni correction) was used to compare SWI and T2*, as well as the respective LMR and ADC among groups.

A multivariate linear model was performed to assess the combined prediction of liver fibrosis with different MR parameters (as T1, T2*, SWI and PDFF).

Bland-Altman analysis was used to evaluate inter-reader agreement for SWI and T2* measurements.

3. Results

3.1. Patient characteristics

Of the 174 patients, 123 patients had normal liver stiffness (shear modulus < 2.8 kPa), 21 had slightly increased liver stiffness (shear modulus 2.8–3.5 kPa) and 30 patients had increased liver stiffness (shear modulus > 3.5 kPa). Patients with a normal liver stiffness were grouped based on the degree of steatosis [30,32]: n = 38 with PDFF < 5%, n = 59 5–10%, n = 19 10–20% and n = 7 > 20% (Fig. 1).

Patient characteristics based on liver stiffness groups are shown in Table 1. Patients with increased liver stiffness were more frequently smokers and consumed more alcohol (both p < 0.001). In patients with increased liver stiffness, various liver-related laboratory parameters were increased (AST, ALT, ALP, Bilirubin, Quick/INR and APRI). When compared to patients with no steatosis, the BMI was significantly

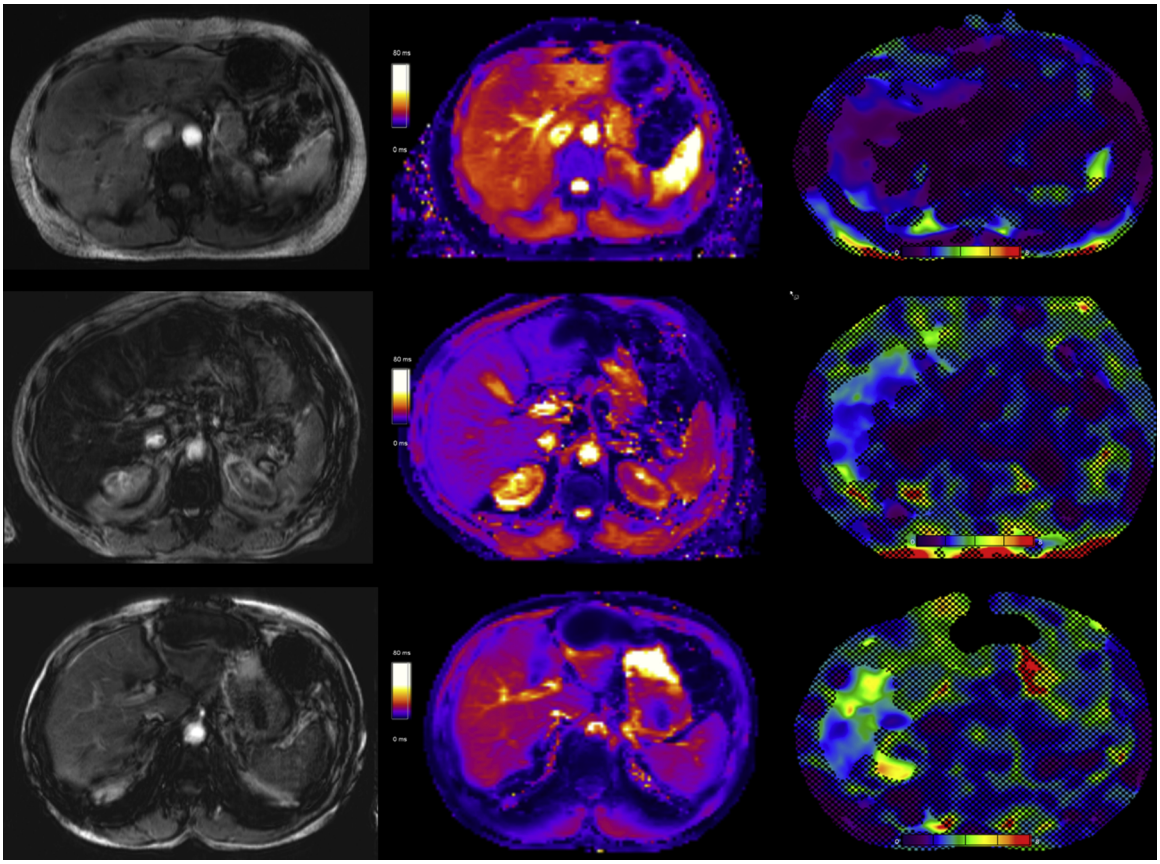

Fig. 4. Patient examples with different amounts of liver steatosis and fibrosis.
In the top row, the SWI image (left display), T2* Map (middle display) and Stiffness Map (right display) of a 24-year-old healthy female subject are shown. The PDFF was 4%, the shear modulus measured on the MR Elastography stiffness map was 1.5 kPa, the signal intensity on the SW images was 167 and the T2* time was 25 ms. In the middle row an example of a patient with steatosis but normal liver stiffness is demonstrated. In this 61-year-old male patient the PDFF was 36%, the shear modulus measured on the MR Elastography stiffness map was 2.6 kPa and the signal intensity on the SW images was 31. The bottom row shows an example of a patient with increased stiffness (3.2 kPa) and minimal steatosis (6%). In this 71-year-old male the signal intensity on SW images was 68 ms and the T2* time was 19 ms.
PDFF = Proton density fat fraction, MR elastography = Magnetic resonance elastography. SW = susceptibility weighted.

higher in patients with a higher degree of liver steatosis (Table 2). In addition, patients with a higher degree of steatosis showed a significantly higher prevalence of diabetes.

3.2. Differentiating the severity of fibrosis

As shown in Table 3 and Fig. 2, the SWI signal intensities and T1 relaxation time values were significantly different ($p < 0.001$) among patients with normal (shear modulus < 2.8 kPa), slightly increased (shear modulus 2.8–3.5 kPa) and at least moderately increased liver stiffness (shear modulus > 3.5 kPa). The T2* values in patients with increased liver stiffness were shorter than in those with normal liver stiffness, as a borderline trend without reaching statistical significance ($p = 0.05$). The SWI, T2* and T1 LMR performed similar to the isolated liver parameters in grading liver fibrosis (Table 3). Mean ADC values were not statistically different between the three groups (< 2.8 kPa: 1188×10^{-6} m/s^2, 2.8–3.5 kPa: 1167×10^{-6} m/s^2, > 3.5 kPa 1154×10^{-6} m/s^2, $p = 0.65$).

3.3. Comparison of different steatosis grades

The results for subjects with normal liver stiffness and different degrees of hepatic fat content are shown in Table 4. The SI on the SWI as well as the T2* relaxation time decreased significantly with an increasing amount of liver fat (both $p < 0.001$), Fig. 3. The SI on SWI was 98 ± 30 and the T2* relaxation time was 22 ± 4 ms in patients with PDFF < 5%, while in patients with PDFF > 20% they were 42 ± 16 and 15 ± 2 ms, respectively. This corresponds to a decrease of about 50% for SWI SI and a third for T2* times, Table 4. Fig. 4 demonstrates these observations in three patient examples with normal findings (upper row), a patient with normal stiffness but steatosis (middle row) and a patient with increased stiffness and only slight steatosis (lower row). Mean ADC values did not show significant difference among patients with different steatosis grades (PDFF < 5%: 1157×10^{-6} m/s^2, 5–10%: 1204×10^{-6} m/s^2, 10–20%: 1174×10^{-6} m/s^2, > 20%: 1141×10^{-6} m/s^2, $p = 0.34$).

3.4. Differentiating the severity of fibrosis depending on different steatosis grades

As shown in Fig. 5, both liver stiffness and steatosis result in decreased SWI and T2* values. While SWI and T2* decrease in patients with increasing degree of liver steatosis, SWI and T2* also decreases in patients with same degree of steatosis but increasing liver stiffness.

3.5. Multivariate linear regression analysis

If PDFF, T1 and age were combined with SWI or T2* in the liver, both were independent predictors for liver fibrosis. A combination of SWI or T2* with age, PDFF and T1 in a multiparametric model showed a multiple r [2] of 0.38 and 0.44, respectively (Table 5).

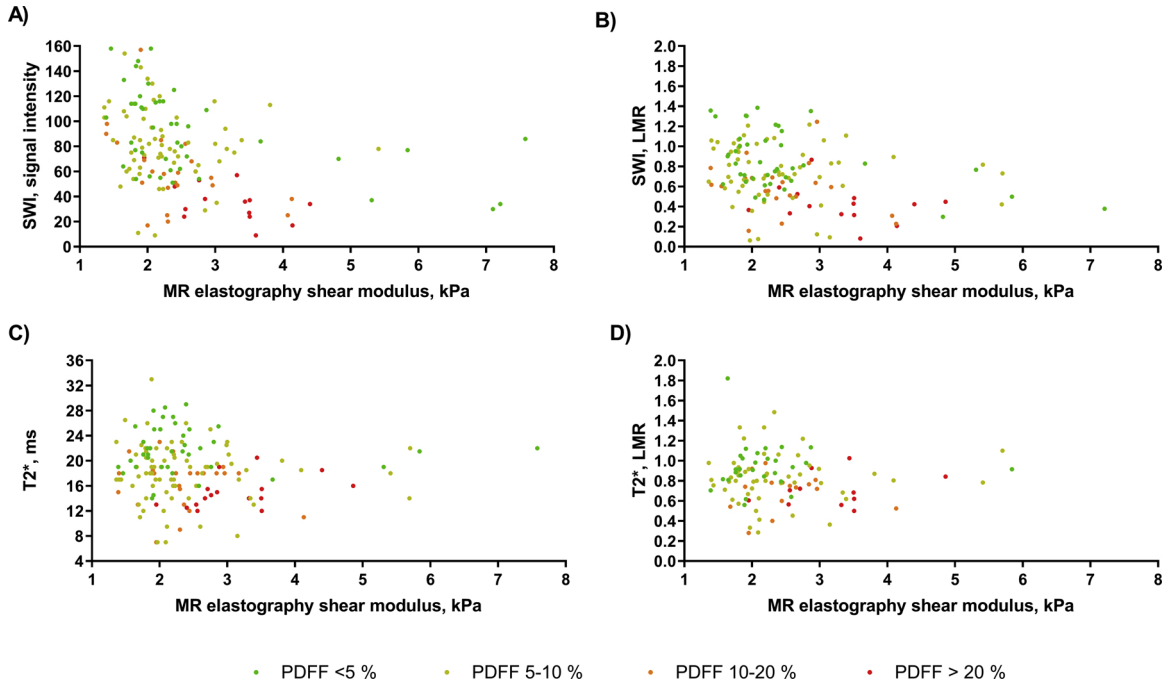

Fig. 5. Correlation of SWI and T2* with MR elastography and PDFF.
Comparison of SI of A) SWI and C) T2* and liver stiffness. Comparison of LMR of B) SWI and D) T2*. Different steatosis grades are color coded with dark green: PDFF < 5%, light green: PDFF 5–10%, orange: PDFF 10–20% and red: PDFF > 20%. For better visibility two patients (Patient 1: Shear modulus 10.5 kPa, PDFF 8%, SWI 36, T2* 21 ms, Patient 2: Shear modulus 16.7 kPa, 1% PDFF, SWI 18, T2* N/A). It is nicely seen that SWI and T2* values decrease from left to right and thus with increasing liver stiffness measured through the shear modulus. Further, there is a clear dominance of green (PDFF < 5%) dots within higher values, while red coded datapoints (PDFF > 20%) all exhibit lower values.
SWI = susceptibility weighted imaging, PDFF = Proton density fat fraction, SI = Signal intensity.

Table 5
Multivariate regression analysis including PDFF, age and T1 for the prediction of liver fibrosis.

	Estimate	Std. Error	t-value	Pr(> |t|)	Multiple r [2]
(Intercept)	−221.49	77.93	−2.84	0.005	0.38
PDFF	−4.75	1.37	−3.46	< 0.001	
age	2.09	0.53	3.94	< 0.001	
SWI	0.63	0.08	7.45	< 0.001	
T1	−1.29	0.29	−4.49	< 0.001	
(Intercept)	−337.56	75.91	−4.45	< 0.001	0.44
PDFF	−6.24	1.45	−4.32	< 0.001	
age	2.21	0.56	3.95	< 0.001	
T2*	0.98	0.10	9.90	< 0.001	
T1	−13.25	2.38	−5.56	< 0.001	
(Intercept)	−243.06	78.03	−3.12	0.002	0.42
PDFF	−6.66	1.55	−4.29	< 0.001	
age	2.23	0.54	4.15	< 0.001	
SWI	0.79	0.10	7.72	< 0.001	
T2*	−1.10	0.31	−3.56	< 0.001	
T1	−5.63	2.67	−2.11	0.037	

Multivariate regression analysis using liver stiffness from MR elastography as reference standard. P-value for all < 0.001.
PDFF = proton density fat fraction, SWI = susceptibility weighted imaging.

3.6. Interreader agreement

Blant Altman-Plots, Fig. 6, show good inter-reader agreement for SWI and T2* with more variation for SWI measurements.

4. Discussion

This study demonstrates that both the SWI and T2* relaxation times are dependent on the presence of liver fat, while SWI is more dependent than T2*. Fat is a known influencing parameter of the T2* relaxation time [13,29,34], but literature on the effect of fat on SWI is sparse. Our results are in a certain discordance with Balassy et al. [24], who reported that SWI LMR did not correlate with steatosis (r = -0.18, p = 0.11 vs. r = -0.47, p < 0.001 in this study). However, Balassy et al. investigated a homogeneous group of patients with mostly advanced fibrosis grades and not much heterogeneity in terms of liver steatosis. Since our results show SWI and T2* dependency of fat, the stage of fibrosis may be overestimated in the presence of steatosis, which should be taken into account when using SWI and T2* in the assessment of fibrosis.

The better performance of SWI alone in separating the degrees of fibrosis than T2* alone (without multiparametric approach) might be explained by the fact that SWI uses both phase and magnitude information [35,36], consisting of an original magnitude image multiplied by a high pass filtered-phase mask image [37]. In contrast, T2* mapping is solely based on the magnitude information but has the advantage of absolute quantification of the T2*-relaxation times. Due to these technical differences, SWI is more susceptibility-weighted than T2* and is therefore more sensitive in detecting hemosiderotic products, which is why it is routinely used to detect microhemorrhages in the brain [38]. Due to its higher susceptibility weighting, SWI might allow better liver fibrosis detection than T2* mapping, as it is able to detect siderotic nodules with a higher sensitivity [39–41]. However, there is evidence of SWI correlating with fibrosis in other organs such as the kidneys [23], suggesting that not only the presence of iron but also alterations of magnetic susceptibility information detected by SWI fibrotic alterations in the interstitial matrix and the inter- and extracellular spaces, liver cell degeneration, necrosis and regeneration are responsible for the observed decrease of SWI signal and T2* relaxation times [26].

In accordance with Balassy et al. [18], our results show that SWI allows noninvasive detection of liver fibrosis. However, we found that direct measurements of SWI signal intensity in the liver performed very

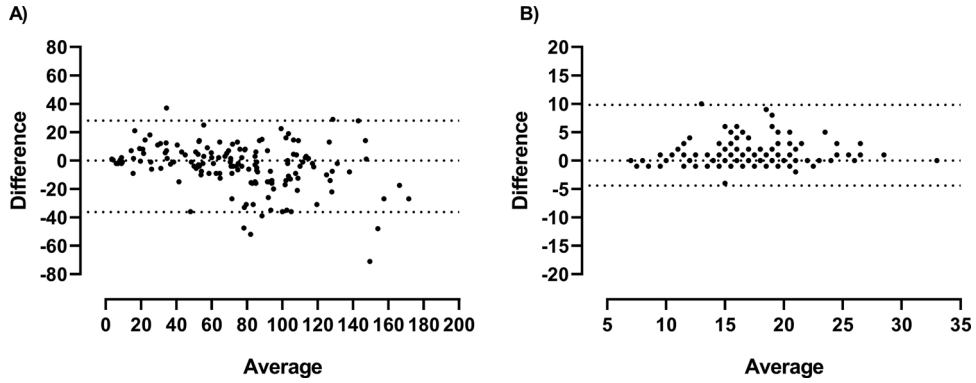

Fig. 6. Bland-Altman plots for both readers.
A) shows differences in the measurements of both readers for SWI and B) for T2*. Dotted lines represent 95% - confidence intervals.

similar to the SWI LMR. While the advantage of T2* in the quantification of liver iron is extensively published in the literature [8,9,42], there are only a few studies describing its value in the assessment of liver fibrosis, mostly in a preclinical setting [43]. One of the few clinical studies showed that the T2* values of the liver allowed for distinguishing patients with liver cirrhosis from healthy controls, which is in accordance with our results [14].

Interestingly, T2* performed better than SWI in staging liver fibrosis when combined in a multiparametric model with the patient's age, PDFF and T1. This might be explained by the hypothesis that T2* measurements are better applicable compared to the SWI relative signal intensities, when the possible confounding steatosis effect is corrected by the PDFF in the multivariate model. Other studies showed the usefulness of multiparametric combinations of MR imaging biomarkers to predict fibrosis, such as the combination of SWI, the apparent diffusion coefficient (ADC) or the relative enhancement after the injection of gadoxetic acid [44]. We therefore believe that both T2* and SWI represent interesting imaging biomarkers that allow a multiparametric combination with other MR techniques for liver tissue characterization.

Our study has several limitations. First, liver biopsy, seen as the best reference standard, was not available in this study due to ethical considerations. To assess liver fibrosis we used MR elastography as the non-invasive reference standard, this allowed us to investigate a general patient population with and without known chronic liver disease. MR elastography has shown excellent accuracy with biopsy-confirmed fibrosis grades [45,46]. Another issue is that T2* decay may no longer be monoexponential in the presence of fat [10]. A multipeak fat spectral modeling of T2* decay might therefore allow a better T2* estimation to predict liver fibrosis [27,47]. Patient numbers in subgroups with both increased liver stiffness and different degrees of steatosis were too small for subgroup analysis. Therefore analysis of the effects of coexisting fibrosis and steatosis is limited. Nevertheless we do see significant influence of fibrosis and steatosis on both SWI and T2*. A follow-up study should therefore calculate cutoff values of SWI and T2* in different histology proven stages of fibrosis, adapted to the degree of steatosis. In higher degrees of steatosis, lower cutoff values of SWI and T2* would be expected than in patients without steatosis to adequately predict fibrosis.

5. Conclusions

In conclusion, SWI- and T2*-mapping are highly dependent on liver steatosis grades. Nevertheless, both parameters are useful predictors for liver fibrosis when using a multiparametric approach. While SWI performed better than T2* in separating patients with and without liver fibrosis, T2* performed slightly better in a multiparametric combination with MR elastography, PDFF, and T1.

Disclosures

There are no disclosures relevant to the manuscript content.

Funding

This work was supported by the Swiss National Science Foundation Research Equipment (R'Equip Grant) and Matching Fund from the University of Bern (Andreas Christe), as well as the foundation to fight against cancer (Adrian Huber).

Acknowledgments

This work was supported by the Swiss National Science Foundation Research Equipment (R'Equip Grant) and Matching Fund from the University of Bern, as well as the foundation to fight against cancer. The authors thank the highly motivated MR imaging technicians and image core lab team from the Department of Diagnostic, Interventional and Pediatric Radiology, Inselspital for their support, especially V. Beutler-Minth, Sarah Gfeller as well as Kathrin Dopke from our study coordination division.

References

[1] J.R. Dillman, A.T. Trout, E.N. Costello, et al., Quantitative Liver MRI-Biopsy Correlation in Pediatric and Young Adult Patients With Nonalcoholic Fatty Liver Disease: Can One Be Used to Predict the Other? AJR Am. J. Roentgenol. 210 (1) (2018) 166–174.
[2] H. Morisaka, U. Motosugi, S. Ichikawa, et al., Magnetic resonance elastography is as accurate as liver biopsy for liver fibrosis staging, J. Magnet. Reson. Imag. 47 (5) (2017) 1268–1275 https://www.ncbi.nlm.nih.gov/pubmed/?term=10.1002%2Fjmri.25868.
[3] A. Srinivasa Babu, M.L. Wells, O.M. Teytelboym, et al., Elastography in chronic liver disease: modalities, techniques, limitations, and future directions, Radiograph. Rev. Pub. Radiolo. Soc. N. Am. Inc. 36 (7) (2016) 1987–2006.
[4] R. Rustogi, J. Horowitz, C. Harmath, et al., Accuracy of MR elastography and anatomic MR imaging features in the diagnosis of severe hepatic fibrosis and cirrhosis, J. Magnet. Reson. Imag. JMRI 35 (6) (2012) 1356–1364.
[5] S.K. Venkatesh, R.L. Ehman, Magnetic resonance elastography of liver, Magn. Reson. Imaging Clin. N. Am. 22 (3) (2014) 433–446.
[6] S. Singh, S.K. Venkatesh, Z. Wang, et al., Diagnostic performance of magnetic resonance elastography in staging liver fibrosis: a systematic review and meta-analysis of individual participant data, Clin. Gastroenterol. Hepatol. Off. Clin. Prac. J. Am. Gastroenterol. Assoc. 13 (3) (2015) 440–451 e446.
[7] P. Kennedy, M. Wagner, L. Castera, et al., Quantitative elastography methods in liver disease: current evidence and future directions, Radiology 286 (3) (2018) 738–763.
[8] R. Labranche, G. Gilbert, M. Cerny, et al., Liver Iron quantification with MR imaging: a primer for radiologists, Radiograph. Rev. Pub. Radiol. Soc. N. Am. Inc. 38 (2) (2018) 392–412.
[9] A. Paisant, A. Boulic, E. Bardou-Jacquet, et al., Assessment of liver iron overload by 3 T MRI, Abdom. Radiol. (NY) 42 (6) (2017) 1713–1720.
[10] T. Yokoo, J.D. Browning, Fat and iron quantification in the liver: past, present, and future, Top. Magnet. Reson. Imag. TMRI 23 (2) (2014) 73–94.
[11] K.V. Kowdley, Iron overload in patients with chronic liver disease, Gastroenterol. Hepatol. (N Y) 12 (11) (2016) 695–698.

[12] Z. Kayali, R. Ranguelov, F. Mitros, et al., Hemosiderosis is associated with accelerated decompensation and decreased survival in patients with cirrhosis, Liver Int. Off. J. Int. Assoc. Study Liver 25 (1) (2005) 41–48.
[13] J.D. Ryan, A.E. Armitage, J.F. Cobbold, et al., Hepatic iron is the major determinant of serum ferritin in NAFLD patients, Liver Int. Off. J. Int. Assoc. Study Liver 38 (1) (2018) 164–173.
[14] D. Wang, T.W. Chen, X.M. Zhang, et al., Liver lobe based multi-echo gradient recalled echo T2*-Weighted imaging in chronic hepatitis B-Related cirrhosis: association with the presence and child-pugh class of cirrhosis, PLoS One 11 (5) (2016) e0154545.
[15] A.R. Guimaraes, L. Siqueira, R. Uppal, et al., T2 relaxation time is related to liver fibrosis severity, Quant. Imaging Med. Surg. 6 (2) (2016) 103–114.
[16] S. Liu, S. Buch, Y. Chen, et al., Susceptibility-weighted imaging: current status and future directions, NMR Biomed. 30 (4) (2017).
[17] J.R. Reichenbach, R. Venkatesan, D.J. Schillinger, D.K. Kido, E.M. Haacke, Small vessels in the human brain: MR venography with deoxyhemoglobin as an intrinsic contrast agent, Radiology 204 (1) (1997) 272–277.
[18] E.M. Haacke, M. Ayaz, A. Khan, et al., Establishing a baseline phase behavior in magnetic resonance imaging to determine normal vs. Abnormal iron content in the brain, J. Magnet. Reson. Imag. JMRI 26 (2) (2007) 256–264.
[19] J. Wu, B. Tarabishy, J. Hu, et al., Cortical calcification in Sturge-Weber Syndrome on MRI-SWI: relation to brain perfusion status and seizure severity, J. Magnet. Reson. Imag. JMRI 34 (4) (2011) 791–798.
[20] J. Zhang, R. Tao, Z. You, et al., Gamna-Gandy bodies of the spleen detected with susceptibility weighted imaging: maybe a new potential non-invasive marker of esophageal varices, PLoS One 8 (1) (2013) e55626.
[21] C. Li, J. Hu, D. Zhou, et al., Differentiation of bland from neoplastic thrombus of the portal vein in patients with hepatocellular carcinoma: application of susceptibility-weighted MR imaging, BMC Cancer 14 (2014) 590.
[22] W. Lv, F. Yan, M. Zeng, J. Zhang, Y. Yuan, J. Ma, Value of abdominal susceptibility-weighted magnetic resonance imaging for quantitative assessment of hepatic iron deposition in patients with chronic hepatitis B: comparison with serum iron markers, J. Int. Med. Res. 40 (3) (2012) 1005–1015.
[23] J.G. Zhang, Z.Y. Xing, T.T. Zha, et al., Longitudinal assessment of rabbit renal fibrosis induced by unilateral ureteral obstruction using two-dimensional susceptibility weighted imaging, J. Magnet. Reson. Imag. JMRI (2017).
[24] C. Balassy, D. Feier, M. Peck-Radosavljevic, et al., Susceptibility-weighted MR imaging in the grading of liver fibrosis: a feasibility study, Radiology 270 (1) (2014) 149–158.
[25] J. Jiang, L. Deng, J. Ruan, X. Cheng, L. Zou, [Value of susceptibility weighted imaging in hepatic fibrosis staging by using MR in a rabbit model], Zhonghua Yi Xue Za Zhi 96 (17) (2016) 1371–1376.
[26] Y. Cai, M.P. Huang, X.F. Wang, X. Lu, L. Luo, J. Shu, Quantitative analysis of susceptibility-weighted magnetic resonance imaging in chronic hepatitis in rats, Magn. Reson. Imaging 54 (2018) 71–76.
[27] J.P. Kuhn, D. Hernando, A. Munoz del Rio, et al., Effect of multipeak spectral modeling of fat for liver iron and fat quantification: correlation of biopsy with MR imaging results, Radiology 265 (1) (2012) 133–142.
[28] M. Franca, A. Alberich-Bayarri, L. Marti-Bonmati, et al., Accurate simultaneous quantification of liver steatosis and iron overload in diffuse liver diseases with MRI, Abdom. Radiol. (NY) 42 (5) (2017) 1434–1443.
[29] M. Karlsson, M. Ekstedt, N. Dahlström, et al., Liver R2* is affected by both iron and fat: a dual biopsy-validated study of chronic liver disease, J. Magn. Reson. Imaging (2019) (0).
[30] J.P. Kuhn, P. Meffert, C. Heske, et al., Prevalence of fatty liver disease and hepatic Iron overload in a northeastern german population by using quantitative MR imaging, Radiology 284 (3) (2017) 706–716.
[31] B.J. Perumpail, M.A. Khan, E.R. Yoo, G. Cholankeril, D. Kim, A. Ahmed, Clinical epidemiology and disease burden of nonalcoholic fatty liver disease, World J. Gastroenterol. 23 (47) (2017) 8263–8276.
[32] G.M. Cunha, K.J. Glaser, A. Bergman, R.P. Luz, E.H. de Figueiredo, Lobo Lopes FPP. Feasibility and agreement of stiffness measurements using gradient-echo and spin-echo MR elastography sequences in unselected patients undergoing liver MRI, Br. J. Radiol. 91 (1087) (2018) 20180126.
[33] S. Singh, S.K. Venkatesh, R. Loomba, et al., Magnetic resonance elastography for staging liver fibrosis in non-alcoholic fatty liver disease: a diagnostic accuracy systematic review and individual participant data pooled analysis, Eur. Radiol. 26 (5) (2016) 1431–1440.
[34] D. Hernando, R.J. Cook, C. Diamond, S.B. Reeder, Magnetic susceptibility as a B0 field strength independent MRI biomarker of liver iron overload, Magn. Reson. Med. 70 (3) (2013) 648–656.
[35] G.B. Chavhan, P.S. Babyn, B. Thomas, M.M. Shroff, E.M. Haacke, Principles, techniques, and applications of T2*-based MR imaging and its special applications, Radiograph. Rev. Pub. Radiol. Soc. N. Am. Inc. 29 (5) (2009) 1433–1449.
[36] R.K. Li, M.S. Zeng, J.W. Qiang, et al., Improving detection of Iron deposition in cirrhotic liver using susceptibility-weighted imaging with emphasis on histopathological correlation, J. Comput. Assist. Tomogr. 41 (1) (2017) 18–24.
[37] E.M. Haacke, Y. Xu, Y.C. Cheng, J.R. Reichenbach, Susceptibility weighted imaging (SWI), Magn. Reson. Med. 52 (2004) 612.
[38] A.L. Cheng, S. Batool, C.R. McCreary, et al., Susceptibility-weighted imaging is more reliable than T2*-weighted gradient-recalled echo MRI for detecting microbleeds, Stroke 44 (10) (2013) 2782–2786.
[39] J. Zhang, G.A. Krinsky, Iron-containing nodules of cirrhosis, NMR Biomed. 17 (7) (2004) 459–464.
[40] Y. Dai, M. Zeng, R. Li, et al., Improving detection of siderotic nodules in cirrhotic liver with a multi-breath-hold susceptibility-weighted imaging technique, J. Magn. Reson. Imaging JMRI 34 (2) (2011) 318–325.
[41] W. Chen, Z. DelProposto, D. Wu, et al., Improved siderotic nodule detection in cirrhosis with susceptibility-weighted magnetic resonance imaging: a prospective study, PLoS One 7 (5) (2012) e36454.
[42] J.M. Alustiza Echeverria, A. Castiella, J.I. Emparanza, Quantification of iron concentration in the liver by MRI, Insights Imaging 3 (2) (2012) 173–180.
[43] A. Muller, K. Hochrath, J. Stroeder, et al., Effects of liver fibrosis progression on tissue relaxation times in different mouse models assessed by ultrahigh field magnetic resonance imaging, Biomed Res. Int. 2017 (2017) 8720367.
[44] D. Feier, C. Balassy, N. Bastati, R. Fragner, F. Wrba, A. Ba-Ssalamah, The diagnostic efficacy of quantitative liver MR imaging with diffusion-weighted, SWI, and hepatospecific contrast-enhanced sequences in staging liver fibrosis–a multiparametric approach, Eur. Radiol. 26 (2) (2016) 539–546.
[45] M. Yin, K.J. Glaser, J.A. Talwalkar, J. Chen, A. Manduca, R.L. Ehman, Hepatic MR Elastography: clinical performance in a series of 1377 consecutive examinations, Radiology 278 (1) (2016) 114–124.
[46] K. Yoshimitsu, T. Mitsufuji, Y. Shinagawa, et al., MR elastography of the liver at 3.0 T in diagnosing liver fibrosis grades; preliminary clinical experience, Eur. Radiol. 26 (3) (2016) 656–663.
[47] S.S. Lee, Y. Lee, N. Kim, et al., Hepatic fat quantification using chemical shift MR imaging and MR spectroscopy in the presence of hepatic iron deposition: validation in phantoms and in patients with chronic liver disease, J. Magn. Reson. Imaging JMRI 33 (6) (2011) 1390–1398.